ISSN 1063-7834, Physics of the Solid State, 2009, Vol. 51, No. 4, pp. 790–796. © Pleiades Publishing, Ltd., 2009.
Original Russian Text © M.V. Gorev, I.N. Flerov, Ph. Sciau, S. Guillemet-Fritsch, 2009, published in Fizika Tverdogo Tela, 2009, Vol. 51, No. 4, pp. 746–752.

MAGNETISM AND FERROELECTRICITY

Thermal Expansion of $(Ba_{1-x}La_x)Ti_{1-x/4}O_3$ Solid Solutions

M. V. Gorev[a, b]*, I. N. Flerov[a, b], Ph. Sciau[c]***, and S. Guillemet-Fritsch[d]**

[a] *Kirensky Institute of Physics, Siberian Branch, Russian Academy of Sciences, Akademgorodok, Krasnoyarsk, 660036 Russia*
**e-mail: gorev@iph.krasn.ru*
***flerov@iph.krasn.ru*
[b] *Siberian Federal University, Svobodnyĭ pr. 79, Krasnoyarsk, 660041 Russia*
[c] *CEMES–CNRS, Université de Toulouse, Toulouse, France*
****e-mail: sciau@cemes.fr*
[d] *CIRIMAT CNRS/UPS/INPT, Université de Toulouse, Toulouse, France*

Received June 10, 2008

Abstract—Deformation and the thermal expansion coefficient of ceramic samples of $(Ba_{1-x}La_x)Ti_{1-x/4}O_3$ solid solutions ($x = 0$, 0.026, 0.036, 0.054) were studied in the temperature range 120–700 K. Based on an analysis of the data obtained, the temperature–composition phase diagram is refined, and the temperature dependence of the polarization is calculated. The results are discussed in combination with the dielectric measurement data.

PACS numbers: 64.70.-p, 65.40.De, 77.84.Dy

DOI: 10.1134/S106378340904026X

1. INTRODUCTION

Barium titanate $BaTiO_3$ is one of the most extensively studied and widely applied materials. At room temperature, it is a ferroelectric with a high permittivity. On heating above the Curie temperature $T_C \approx 400$ K, it undergoes a phase transition to the paraelectric cubic phase $Pm3m$. In order to modify the electrical properties of $BaTiO_3$, cation doping is used into both sites *A* and *B* of the perovskite lattice [1–5].

Isovalent doping into sites *B* is commonly used to change the temperature T_C and the lower temperatures of the phase transitions from the tetragonal to orthorhombic phase (T_1) and from the orthorhombic to rhombohedral phase (T_2). For example, the doping with nonferroelectric ions Zr^{4+} and Sn^{4+} leads to a linear decrease in the temperature T_C and an increase in the temperatures T_1 and T_2 [4, 6]. As the concentration of a doping ion increases in many such systems, the tetragonal and orthorhombic phases wedge out and then the crossover occurs from the usual ferroelectric to relaxor behavior [6]. Isovalent doping does not have a substantial influence on the charge state and does not cause the appearance of random electric fields. However, the Zr^{4+} ion is ~20% larger in size than the Ti^{4+} ion in six-coordinated surroundings; such substitution must lead to the formation of random elastic fields and is likely to be responsible for the appearance of relaxor properties in $BaTi_{1-x}Zr_xO_3$ at $x > 0.25$ [6].

Heterovalent substitution of trivalent bismuth for Ba^{2+} has practically no influence on the temperature T_C up to concentrations of ~10%. However, at a bismuth content of 2%, the permittivity anomalies at T_1 and T_2 coalesce into one anomaly, which arises in the ferroelectric state and is characterized by substantial frequency dispersion [7]. It is believed that the difference between the valences of Ba^{2+} and Bi^{3+} is responsible for the formation of random electric fields, destruction of the ferroelectric order, and the occurrence of the relaxor state at high Bi concentrations.

Contrary to bismuth, an addition of trivalent lanthanum quickly decreases the temperatures T_C, T_1, and T_2 [8, 9]. At heterovalent substitution for barium, the charge compensation can be due to the formation of barium vacancies, as in the case of bismuth doping (compounds $Ba_{1-x}\square_{x/3}Bi_{2x/3}TiO_3$) [7] or due to the formation of titanium vacancies, as in the case of lanthanum doping (compounds $Ba_{1-x}La_xTi_{1-x/4}\square_{x/4}O_3$) [9]. In the latter case, the doping changes ferroelectrically active sites *B* of the lattice (as in the case of doping with zirconium) and thereby substantially changes the temperatures of ferroelectric phase transitions. At La concentrations of ~4–10%, relaxor phenomena take place, which may be due to the formation of La^{3+}-ion and Ti-vacancy clusters and the appearance of strong random electric fields destroying the uniform ferroelectric state [9].

Many aspects of the phenomena occurring in these materials still remain unclear and require additional studies. The thermal expansion is one of the main properties and is related to many important (ferroelectric, piezoelectric, and pyroelectric) properties of the mate-

rials. Moreover, the primary order parameter in barium titanate and its derivatives is the polarization due to ion displacements, and phase transitions can be detected by measuring the thermal expansion because macroscopic deformation is related to microscopic lattice deformation. A knowledge of the thermal expansion is necessary for designing various technological devices and for elucidating the physical origin of phenomena occurring in solid solutions, such as the crossover from the usual ferroelectric to relaxor behavior.

In this work, the thermal expansion of ceramic samples of $Ba_{1-x}La_xTi_{1-x/4}O_3$ (x = 0, 0.026, 0.036, 0.054) was measured to refine the temperature–composition phase diagram. Moreover, we determined the behavior of the root-mean-square (rms) polarization and its dependence on the lanthanum concentration from the data on the thermal expansion, since a direct measurement of the polarization of ceramic materials by traditional methods is often hampered.

2. EXPERIMENTAL

The $Ba_{1-x}La_xTi_{1-x/4}O_3$ compounds (x = 0, 0.026, 0.036, 0.054) were prepared by the method described in [10, 11] from $BaCl_2 \cdot 2H_2O$, $TiCl_3$, and $LaCl_3 \cdot 7H_2O$. A solution of oxalic acid in ethanol was added to an aqueous solution of the primary reagents. The reaction proceeded for 2 h, thereafter a precipitate was separated in a centrifuge. To obtain oxides, the intermediate compounds were subjected to hydrolysis at 850°C for 4 h. Samples in the form of pellets 6 mm in diameter and 2–4 mm thick were prepared by compacting powders with addition of an organic binder at 250 MPa [10].

The chemical composition of the samples and their structure were determined on an ICP AES Thermo-Optec ARL 3580 plasma spectrometer and by X-ray diffraction analysis (SEIFERT XRD-3003-TT diffractometer, CuK_α radiation, λ = 0.15418 nm). The results are given in the table. The pure $BaTiO_3$ produced by codeposition at room temperature is tetragonal, while the compounds doped with La^{3+} ($x \geq 0.026$) have a cubic structure.

Thermal expansion was measured by a NETZSCH DIL-402C dilatometer over the temperature range 120–700 K in a dynamic regime at a heating rate of 5 K/min. In order to perform calibration and take into account the thermal expansion of the measuring system, reference samples of fused quartz and corundum were used.

For different samples of the same composition (see table), several series of measurements were carried out. The results, as a rule, coincide to within the error of measurement

Parameters of samples

x	Compound	Density, %	Structure at 300 K
0	$BaTiO_3$	95.5	Tetragonal
0.026	$Ba_{0.974}La_{0.026}Ti_{0.993}O_3$	90.0	Cubic
0.036	$Ba_{0.964}La_{0.036}Ti_{0.991}O_3$	90.7	"
0.054	$Ba_{0.946}La_{0.054}Ti_{0.986}O_3$	92.1	"

3. RESULTS AND DISCUSSION

3.1. $BaTiO_3$

The results of measurements of the strain $\Delta L/L(T)$ and the thermal expansion coefficient $\alpha(T)$ for a ceramic sample of pure $BaTiO_3$ are presented in Fig. 1. Anomalies of $\alpha(T)$ due to the phase transitions $Pm3m \longrightarrow P4mm \longrightarrow C2mm \longrightarrow R3m$ are observed at temperatures T_C = 401.8 K, T_1 = 299.5 K, and T_2 = 216.1 K. The anomalies at T_1 and T_2 are split, which may be due to an inhomogeneity and the ceramic nature of the sample. The measured values of the thermal expansion coefficient agree well with the data from [12, 13], especially above the transition temperature between the cubic and tetragonal phases.

From the thermodynamic theory of phase transitions, it follows that the strain in $BaTiO_3$ is mainly determined by the squared polarization

$$\frac{\Delta L}{L} = \int \alpha_L(T)dT + (Q_{11} + 2Q_{12})\langle P^2\rangle, \qquad (1)$$

where $\alpha_L(T)$ is the thermal (not anomalous) expansion coefficient of the lattice and Q_{11} and Q_{12} are the electrostriction coefficients. Equation (1) can be used to estimate the spontaneous macroscopic polarization of ferroelectrics and the dynamic polarization of ferroelectric relaxors. This dependence is also frequently used to determine the Burns temperature T_d [12, 14–16].

To separate the anomalous contribution $(Q_{11} + 2Q_{12})\langle P^2\rangle$ to the strain and determine the polarization P, it is necessary to correctly describe the anomaly-free contribution to the strain and the thermal expansion coefficient $\alpha_L(T)$. We estimated the rms polarization using three different procedures of approximating the lattice strain and separating the anomalous contribution. The results are presented in Fig. 2 together with the data from [17] obtained for the tetragonal phase of the crystal from dielectric hysteresis loops. Figure 2 also shows the temperature dependence of the polarization estimated in [18] from data on the heat capacity of a 100-nm-thick film of $BaTiO_3$. The polarization was calculated assuming that the electrostriction constants Q_{11} and Q_{12} [19, 20] are independent of temperature.

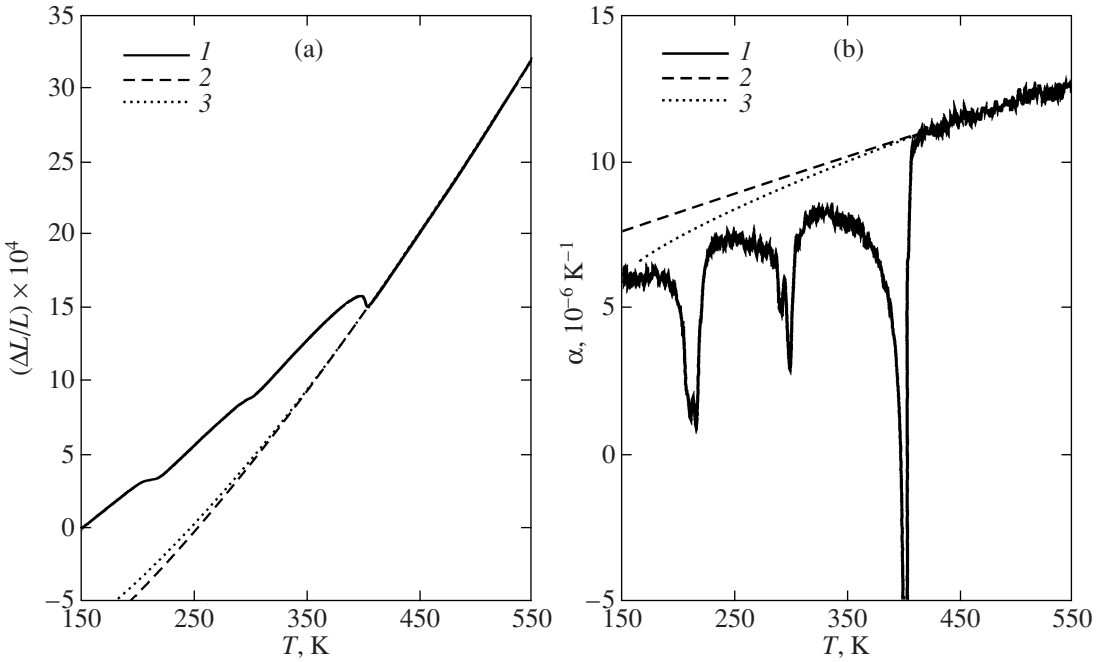

Fig. 1. Temperature dependences of (a) the strain and (b) thermal expansion coefficient of $BaTiO_3$: (*1*) experimental data, (*2*) fitting of the anomaly-free contribution by Eq. (3), and (*3*) fitting by Eq. (4).

In the first procedure, we used the traditional approach [14–16] in which the elongation $\Delta L/L(T)$ at high temperatures is fitted by a linear dependence

$$\Delta L/L(T) = a + bT. \quad (2)$$

It is assumed that the temperature of deviation from this dependence corresponds to the Burns temperature T_d, at which polar nanoscopic regions begin to arise in a sample. However, the values of T_d thus determined, the anomalous contribution, and the rms polarization are, as a rule, overestimated and dependent on the temperature range over which the fitting is performed [12]. Moreover, even in the compounds wherein the polar phase is principally impossible, the temperature dependence of $\Delta L/L(T)$ is noticeably nonlinear and, therefore, the thermal expansion coefficient $\alpha(T)$ is not constant. In $BaTiO_3$ at temperatures $T > T_C$, the strain is poorly described by a linear dependence and the rms polarization is clearly overestimated when one goes away from T_C to low temperatures (Fig. 2, curve *3*).

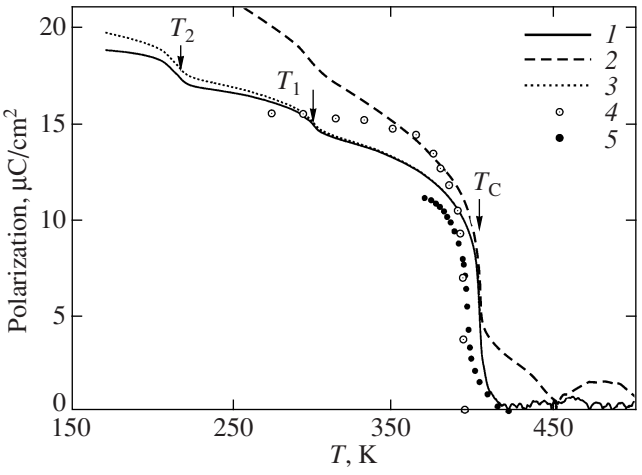

Fig. 2. Temperature dependences of the polarization of $BaTiO_3$ obtained by fitting the strain with (*1*) Eq. (4), (*2*) Eq. (3), and (*3*) linear dependence (2); (*4*) the data from [18] and (*5*) the data from [17].

According to the Grüneisen theory of thermal expansion, the thermal expansion coefficient is slightly dependent on temperature above the Debye temperature, which causes the strain to be nonlinear. Moreover, at high temperatures, there are additional contributions to the strain due to thermally induced defects, which is also demonstrated by the high-temperature behavior of the thermal expansion coefficient $\alpha(T)$. At high temperatures, the $\alpha(T)$ of barium titanate is practically linear in temperature [12]

$$\alpha(T) = a + bT. \quad (3)$$

The inclusion of these contributions significantly improves the fitting of the temperature dependences of $\alpha(T)$ and the strain at $T > T_C$ and decreases the polarization at low temperatures (Fig. 2, curve *2*). However, this approach is also incorrect. As the temperature decreases, the thermal expansion coefficient must tend to zero and, in order to estimate the polarization at low temperatures ($T < T_C < \Theta_D$), it is necessary to include the relation between the thermal expansion and the heat

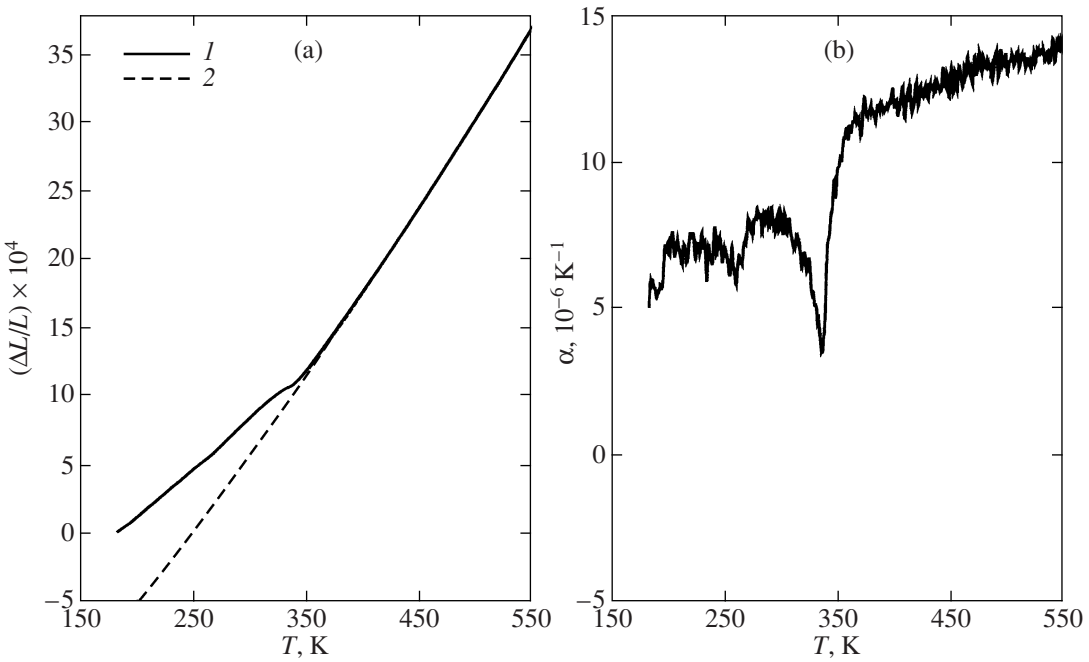

Fig. 3. Temperature dependences of (a) the strain and (b) thermal expansion coefficient of $Ba_{1-x}La_xTi_{1-x/4}O_3$ at $x = 0.026$: (*1*) experimental data and (*2*) fitting of the anomaly-free contribution by Eq. (3).

capacity and its temperature dependence, at least in terms of the Debye model.

Since the thermal expansion coefficient of the cubic phase (at $T > T_C \approx \Theta_D$) is slightly dependent on temperature and the determination of the Debye temperature from fitting the experimental data is practically impossible, we used the averaged value $\Theta_D \approx 432$ K [21]. The data were processed by the dependence

$$\alpha(T) = aT + bC_D(T). \quad (4)$$

Here, a and b are adjustable parameters and

$$C_D(T) = 9R\left(\frac{\Theta_D}{T}\right)^3 \int_0^{\Theta_D/T} t^4 \frac{\exp(t)}{(\exp(t)-1)^2} dt = 3R\left[4D_3(x_D) - \frac{3x_D}{\exp(x_D)-1}\right], \quad (5)$$

where $x_D = \Theta_D/T$ and $D_3(x_D)$ is the third-order Debye function. The results of processing the experimental data with Eq. (5) for $BaTiO_3$ are shown in Fig. 1 (curve *3*), and the polarization calculated from Eq. (1) is presented in Fig. 2 (curve *1*). In our opinion, this procedure of separating the anomalous contribution to the strain and determining the polarization is more correct.

In what follows, for all solid solutions, this approach is used to separate the anomalous contribution to the strain and the thermal expansion coefficient and calculate the polarization.

3.2. $Ba_{1-x}La_xTi_{1-x/4}O_3$ *Solid Solutions*

The results of the study of the solid solutions are presented in Figs. 3–5. As the lanthanum concentration increases, the anomaly of $\alpha(T)$ at T_C becomes smaller, but remains fairly sharp and is easily detected at $x = 0.026$ and 0.036. The pretransition phenomena above T_C are more pronounced, which is indicative of structural inhomogeneity and a distribution of transition temperatures over the bulk of the sample. The anomalies at T_1 and T_2 decrease and are spread significantly faster. Even at $x = 0.036$, they practically coalesce and form a shoulder on the low-temperature side of the anomaly at T_C. For all compositions, the anomalous component of $\alpha(T)$ in the cubic phase arises at approximately the same temperature $T_d \approx 400$–420 K.

The behavior of the anomalous component of the thermal expansion coefficient α correlates with that of the permittivity ε [8, 9].

3.3 Phase Diagram of the $Ba_{1-x}La_xTi_{1-x/4}O_3$ *System*

The phase diagram of the system is shown in Fig. 6, where, along with the data obtained from the thermal expansion, the results of measuring the dielectric properties [8, 9] are presented. Over the concentration range studied, the data on T_C and T_1 agree well. However, unlike [8], we did not observed a noticeable increase in T_2 with concentration and wedging-out of the *C*2*mm* phase.

As noted in Section 1, the phase diagrams of solid solutions with trivalent lanthanum and trivalent

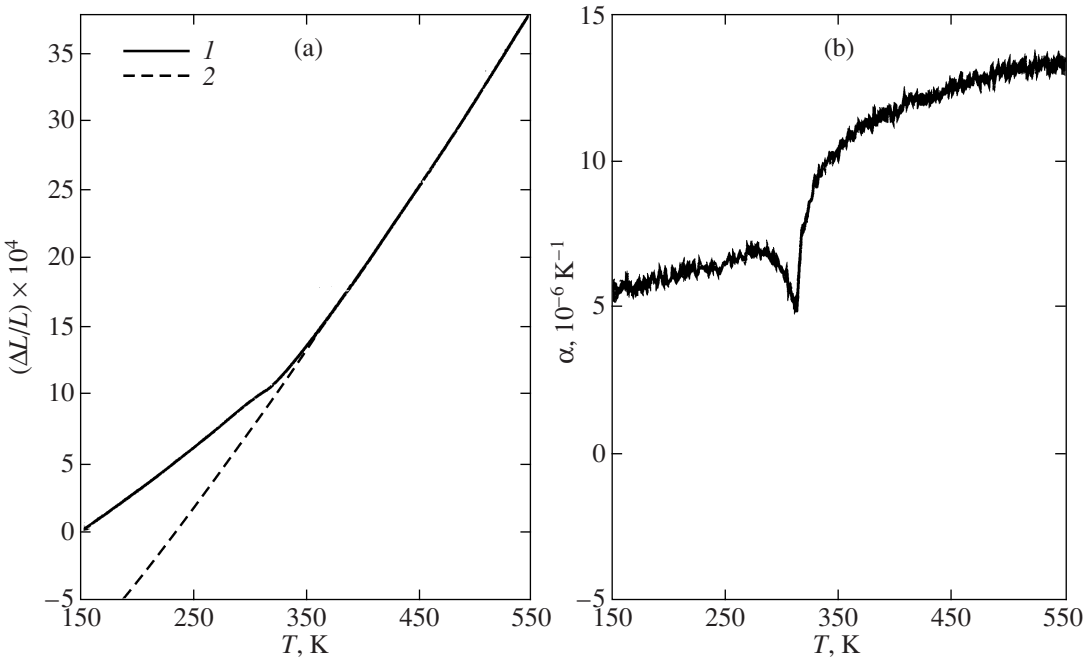

Fig. 4. Temperature dependences of (a) the strain and (b) thermal expansion coefficient of $Ba_{1-x}La_xTi_{1-x/4}O_3$ at $x = 0.036$: (*1*) experimental data and (*2*) fitting of the anomaly-free contribution by Eq. (3).

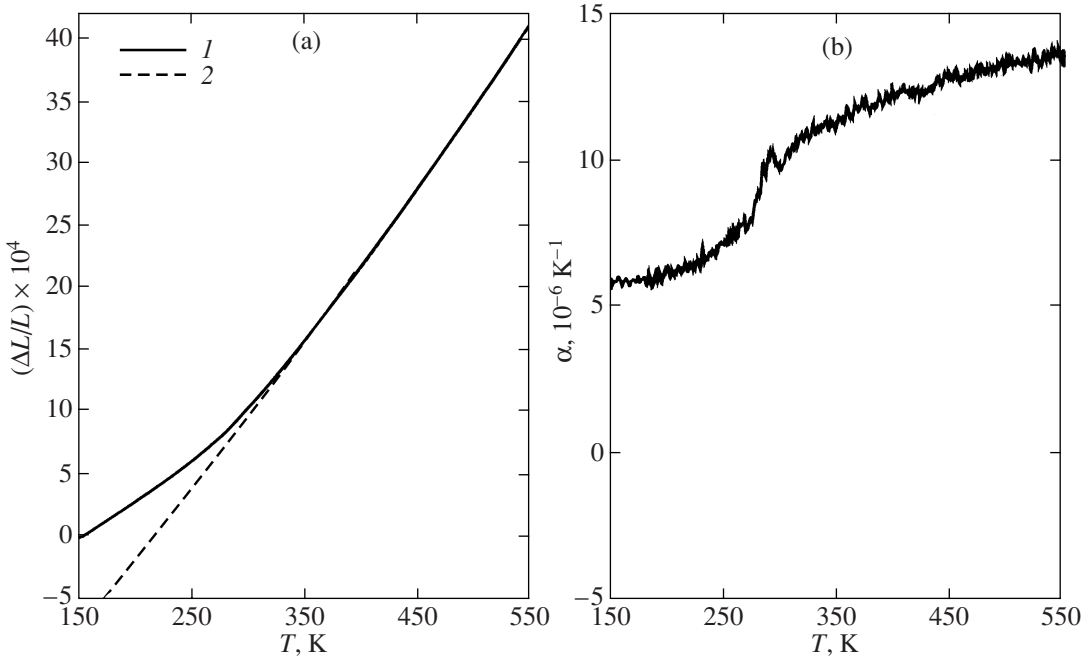

Fig. 5. Temperature dependences of (a) the strain and (b) thermal expansion coefficient of $Ba_{1-x}La_xTi_{1-x/4}O_3$ at $x = 0.054$: (*1*) experimental data and (*2*) fitting of the anomaly-free contribution by Eq. (3).

bismuth substituted for barium are different. This circumstance may be due to different mechanisms of charge compensation. When bismuth is added, the compensation is due to the formation of barium vacancies, which leads to the compound $Ba_{1-x}\square_{x/3}Bi_{2x/3}TiO_3$ [6]. Calculations of the lattice energy showed that, when lanthanum substitutes for barium, the charge compensation is due to the formation of titanium vacancies (the compound $Ba_{1-x}La_xTi_{1-x/4}\square_{x/4}O_3$) [9, 22]. In the latter case, the

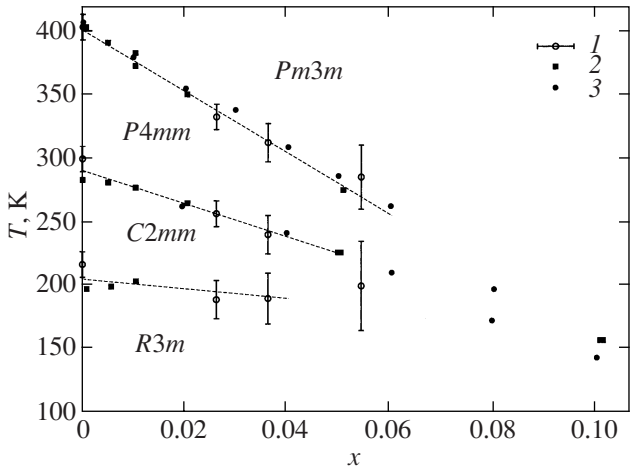

Fig. 6. Phase diagram of the $Ba_{1-x}La_xTi_{1-x/4}O_3$ system: (*1*) dilatometric data, (*2*) data from [8], and (*3*) data from [9].

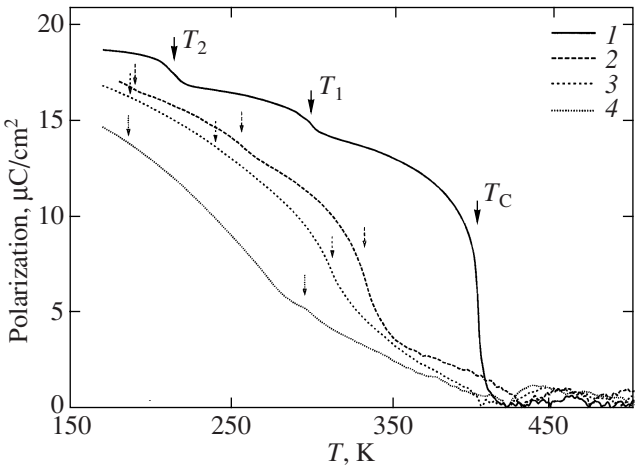

Fig. 7. Temperature dependence of the polarization of $Ba_{1-x}La_xTi_{1-x/4}O_3$ for various values of x: (*1*) 0, (*2*) 0.026, (*3*) 0.036, and (*4*) 0.054.

doping causes changes in the ferroelectrically active sites B of the perovskite lattice and thereby substantially changes the temperatures of ferroelectric phase transitions, as in the $BaTi_{1-x}M_xO_3$ systems (M = Zr, Sn, etc.) [4, 6].

According to [7], the bismuth doping causes wedging-out of the *C*2*mm* phase and the occurrence of unusual relaxor phenomena at T_m in the ferroelectric state. It is not inconceivable that such phenomena are also caused by lanthanum doping. However, the intervals between the phase transition temperatures in this case are significantly smaller and it is much more difficult to determine T_1, T_2, and T_m because of substantial spreading and overlapping of the anomalies in the concentration range $x = 0.036$–0.100. Nevertheless, even at a La concentration $x \sim 0.04$ and temperatures $T < T_C$, noticeable dispersion ε and relaxor phenomena were observed in [9], which were enhanced with increasing concentration x.

Relaxor phenomena in compounds in which barium is heterovalently substituted by (in particular) lanthanum are related to the formation of La^{3+}-ion and Ti-vacancy clusters and the appearance of strong random electric fields destroying the uniform ferroelectric state [9].

3.4. Polarization

The temperature dependence of polarization calculated from the strain of ceramic samples is shown in Fig. 7. For $Ba_{1-x}La_xTi_{1-x/4}O_3$ solid solutions, we used the same electrostriction coefficients as for $BaTiO_3$.

As the lanthanum concentration increases, the appearance of polarization is more and more spread and it exists over a wide temperature range above T_C. The deviation of the strain from a regular behavior and the appearance of nonzero polarization in the solid solutions are observed at temperatures near ~420 K, which significantly exceed the transition temperature to the ferroelectric phase T_C. Such deviations below the Burns temperature T_d are due to the appearance of polar nanoregions with randomly oriented polarization in the paraelectric phase and have been observed in ferroelectrics $BaTiO_3$, $PbTiO_3$, and $KNbO_3$ and ferroelectric relaxors when studying various physical properties [14]. For example, in $BaTi_{1-x}Sn_xO_3$ solid solutions, the Burns temperature increases with Sn concentration [12]. In our case, the Burns temperature remains almost unchanged; however, the temperature T_C decreases significantly faster than in $BaTi_{1-x}Sn_xO_3$, so that the difference $T_d - T_C$ varies linearly with increasing lanthanum concentration from ~10 K at $x = 0$ to ~150 K at $x = 0.054$.

4. CONCLUSIONS

Thus, in this study, we have revealed the anomalous behavior of the strain and the thermal expansion coefficient of ceramic materials $Ba_{1-x}La_xTi_{1-x/4}O_3$ and have refined the T–x phase diagram for them. It was established that the temperature dependence of the thermal expansion (strain) is nonlinear, and a method was proposed for determining the root-mean-square polarization from the dilatometric data.

ACKNOWLEDGMENTS

This work was supported by the Russian Foundation for Basic Research (project no. 07-02-00069) and the Council on Grants from the President of the Russian Federation for the Support of Leading Scientific Schools of the Russian Federation (grant NSh-1011.2008.2).

REFERENCES

1. D. Hennings, A. Schnell, and G. Simon, J. Am. Ceram. Soc. **65**, 539 (1982).
2. J. Ravez and A. Simon, Eur. J. Solid State Inorg. Chem. **34**, 1199 (1997).
3. R. Farhi, M. El. Marssi, A. Simon, and J. Ravez, Eur. Phys. J. B **9**, 599 (1999).
4. C. Ang, Z. Jing, and Z. Yu, J. Mater. Sci. **38**, 1057 (2003).
5. J. Ravez and A. Simon, Phys. Status Solidi A **178**, 793 (2000).
6. A. Simon, J. Ravez, and M. Maglione, J. Phys.: Condens. Matter **16**, 963 (2004).
7. A. Simon, J. Ravez, and M. Maglione, Solid State Sci. **7**, 925 (2005).
8. M. Kchikech and M. Maglione, J. Phys.: Condens. Matter **6**, 10159 (1994).
9. F. D. Morrison, D. C. Sinclair, and A. R. West, J. Appl. Phys. **86**, 6355 (1999).
10. M. Boulos, S. Guillemet-Fritsch, Q. Nguyen, Z. Valdez-Nava, J. Farenc, and B. Durand, Silic. Ind. (in press).
11. K. Aliouane, A. Guehria-Laidoudi, A. Simon, and J. Ravez, Solid State Sci. **7**, 1324 (2005).
12. V. Mueller, L. Jager, H. Beige, H.-P. Abicht, and T. Muller, Solid State Commun. **129**, 757 (2004).
13. Y. He, Thermochim. Acta **419**, 135 (2004).
14. G. Burns and F. H. Dacol, Phys. Rev. B: Condens. Matter **28**, 2527 (1983).
15. A. S. Bhalla, R. Guo, L. E. Cross, G. Burns, F. H. Dacol, and R. R. Neurgaonkar, Phys. Rev. B: Condens. Matter **36**, 2030 (1987).
16. S. Wongsaenmai, R. Yimnirun, S. Ananta, R. Guo, and A. S. Bhalla, Mater. Lett. **62**, 352 (2008).
17. W. J. Merz, Phys. Rev. **76**, 1221 (1949).
18. B. A. Strukov, S. T. Davitadze, S. N. Kravchuk, S. A. Taraskin, M. Goltzman, V. V. Lemanov, and S. G. Shulman, J. Phys.: Condens. Matter **15**, 4331 (2003).
19. G. A. Smolenskiĭ, V. A. Bokov, V. A. Yusupov, N. N. Kraĭnik, R. E. Pasynkov, and M. S. Shur, *Ferroelectrics and Antiferroelectrics* (Nauka, Leningrad, 1971) [in Russian].
20. S. Nomura and K. Uchino, Ferroelectrics **41**, 117 (1982).
21. W. N. Lawless, Phys. Rev. B: Solid State **17**, 1458 (1978).
22. F. D. Morrison, A. M. Coats, D. C. Sinclair, and A. R. West, J. Electroceram. **6**, 219 (2001).

Translated by Yu. Ryzhkov